Selective Reduction of Phosphorus from Manganese Ore to Produce Ferromanganese Alloy with Low Phosphorus Content

Dong Jun Shin[1] · Xu Gao[2] · Shigeru Ueda[2] · Shin-ya Kitamura[2]

Abstract

The authors proposed the selective reduction of P from steelmaking slag to enable the recycling of steelmaking slag for the sintering process, and for the extraction of P and Mn separately. By decreasing the basicity of the slag and increasing the temperature of the reduction, Fe and P were reduced to the metal, while most of the Mn remained in the slag. In this study, this selective reduction technique was applied to a kind of Mn ore to remove P. The influences of the different mixing ratios of graphite, SiO_2, and pig iron as well as the temperature on the reduction behavior were investigated. By adding SiO_2 as a slag modifier to produce an acidic slag with a low melting temperature and adding graphite and pig iron as a reductant and receiver, respectively, the selective reduction of P without the reduction of Mn was achieved for Mn ore. When the slag obtained after the selective reduction of Mn ore was used in the smelting reduction process to produce the ferromanganese alloy, a significant decrease in the P content of ferromanganese was estimated through a mass balance calculation. Therefore, the selective reduction of P from Mn ore has the potential to produce high-grade ferromanganese alloys with low P content.

Keywords Mn ore · Selective reduction · Ferromanganese alloy · Low phosphorus

Introduction

Manganese is an important alloying element for steel. As a result of the increasing demand for high-performance steel with high strength and ductility, the Mn content of steel is being increased. On the other hand, to improve ductility and suppress embrittlement, steel with low P content is necessary. Because Mn is added as ferroalloy containing approximately 0.2−0.4 mass% P [1–3], the P content of steel inevitably increases when producing steel with high Mn content. In the case of ultrahigh Mn steel, (e.g., twinning-induced plasticity (TWIP) steel or nonmagnetic steel), the increase in P content with the alloy addition is unacceptable [4, 5],

and thus an expensive metallic Mn produced by electrolysis is used. Therefore, the demand for low P-containing ferromanganese is expected to increase.

Ferromanganese alloys are produced through the reduction of manganese ore in either electric furnaces or blast furnaces. As almost all of the P content in the raw material is distributed into the molten metal in this reduction process, the P content in the ferroalloy is completely controlled by the P content of the raw materials, particularly the manganese ore.

To decrease the P content, oxidation refining of the ferromanganese alloy has been investigated. As Mn is easily oxidized by conventional dephosphorization using a CaO-based slag, a considerable amount of Mn can be oxidized without any marked decrease in the P content. Subsequently, a BaO-based slag was investigated by several researchers. For example, Chaudhary et al. [6] conducted dephosphorization of a high-carbon ferromanganese alloy without significant loss of Mn by using a $BaCO_3$–BaF_2-based flux. Fujita et al. [7] demonstrated the high phosphate capacity of a BaO-based flux by conducting dephosphorization of a high-carbon Fe–Mn alloy. Shim et al. [8] and Watanabe et al. [9] reported equilibrium data between a BaO–BaF_2–MnO slag and a high-carbon Fe–Mn alloy, and showed the effect

✉ Xu Gao
gao@tohoku.ac.jp

1 Department of Metallurgy, Graduate School of Engineering, Tohoku University, 2-1-1 Katahira, Aoba-ku, Sendai 980-8577, Japan

2 Institute of Multidisciplinary Research for Advanced Materials, Tohoku University, 2-1-1 Katahira, Aoba-ku, Sendai 980-8577, Japan

of adding BaF_2 to a BaO-based flux. Liu et al. [10] investigated the influence of additives to a $BaO–BaF_2–MnO$ slag on the distribution of P and Mn between the slag and a high-carbon Fe–Mn alloy. However, owing to the high price of the flux and severe damage to the refractory lining of the vessel, this slag is not used in industry. In addition, Kim et al. [11] studied the behavior of phosphorus during the formation of a (Mn, Fe)-carbide, by a carbothermal solid-state reduction of Mn ore [12, 13].

The application of mineral dressing to remove P has also been investigated. Rao et al. [14] and Acharya et al. [15] showed that P was preferentially observed in the goethite phase in Mn ore and attempted a magnetic separation using the difference in magnetic properties between goethite and the other phases. The concentration of Mn in the nonmagnetized ore was enriched to 40 mass% from 32 mass%, while the P content was decreased to 0.3 mass% from 0.45 mass% (all the compositions in this paper are given in mass percentage, unless otherwise specifically stated).

Hils et al. [16] reported a method to produce a $MnO–SiO_2$ slag with low P as the raw material for a Si–Mn alloy. A mixture of the Mn ores, iron ore, coke, and SiO_2 was reduced at 1373 K, after which the temperature was raised to melt the sample for phase separation. The Fe and P in the ore were reduced to produce hot metal, and the P content of the separated slag in the $MnO–SiO_2$ system was relatively low. The slag was used as a raw material for Si–Mn alloy production, and the P content in the Si–Mn was less than 0.02%.

Previously, we proposed the selective reduction of P from steelmaking slag to enable the recycling of steelmaking slag for the sintering process, and for the extraction of P and Mn separately [17–21]. By decreasing the basicity of the slag and increasing the temperature of the reduction, Fe and P were reduced to the metal, while most of the Mn remained in the slag. The results at the optimal conditions showed that the highest removal ratio of P from the slag was more than 95%, while the loss of Mn to the metal was less than 5%.

In this study, the selective reduction technique is applied to a kind of Mn ore to remove P. The influences of the different mixing ratios of graphite, SiO_2, and pig iron and the effect of the temperature on the reduction behavior were investigated. The possibility of producing ferromanganese with low P after selective reduction was discussed.

Experimental

Characteristics of the Mn Ore

Mn ore with a particle size of less than 2 mm was used in this study. The crystalline phases present in the ore were identified using X-ray diffraction (XRD) and are shown in Fig. 1. In the natural state of the Mn ore, Mn and Si existed
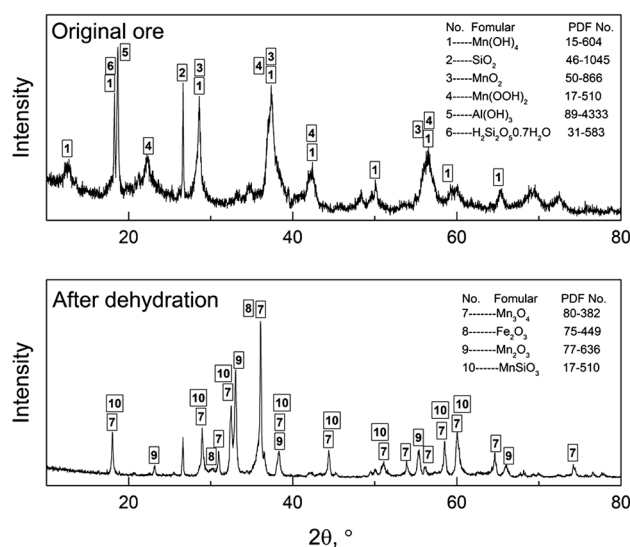

Fig. 1 Mineralogical phases of the natural Mn ore before and after dehydration

in both oxide and hydroxide forms, while Al was observed mainly as a hydroxide. The rapid evaporation of the hydrated compound during heating leads to a large volume expansion. Therefore, the hydrated compound in Mn ore was removed prior to the reduction experiment by heat treatment at 1273 K for 1 h in air. The changes in the crystalline phases of the Mn ore after dehydration are also shown in Fig. 1. After dehydration, the hydroxides were transformed to oxides, forming $MnSiO_3$ as a result of the reaction between Mn oxides and SiO_2 during the heat treatment. In addition, the valence state of Mn in the oxide was changed during the heat treatment, but this change was not considered to affect the reduction behavior. This is because the reduction was expected to occur in the molten state, and Mn^{2+} becomes the stable cation in molten slag when coexisting with hot metal.

The chemical composition of the Mn ore was analyzed using inductively coupled plasma atomic emission spectroscopy (ICP–AES) and is listed in Table 1, where "T" indicates the total content, as the valence states of these oxides were not identified.

Design of Slag Composition and Experimental Conditions

According to prior studies on steelmaking slag, designing an acidic slag with a low melting point is key for selectively reducing P into the metal while suppressing the reduction of Mn [21]. Thus, SiO_2 was chosen as the slag modifier. Although various Mn oxides exist with different valence states (e.g., MnO_2, Mn_2O_3, and Mn_3O_4), MnO is considered to be stable during the state of smelting reduction. In addition, most of the Fe oxide in the Mn ore is

Table 1 Chemical compositions of the Mn ore before and after dehydration (mass%)

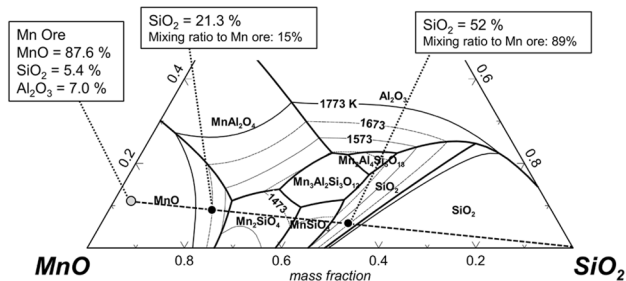|	T. Fe	T. Mn	SiO_2	Al_2O_3	T. P	Others (Ca, Mg, Cr, S)
Natural state	3.43	52.31	4.12	6.58	0.14	< 0.5
After dehydration	3.26	65.84	5.21	6.83	0.15	< 0.5

Fig. 2 Isothermal liquid composition line of the MnO–SiO_2–Al_2O_3 slag system calculated using FactSage

reduced rapidly, and thus the Fe oxide content of the Mn ore does not need to be considered. Therefore, the major composition of the Mn ore can be simplified to the ternary system of MnO–SiO_2–Al_2O_3. Figure 2 shows the liquidus area of the MnO–SiO_2–Al_2O_3 system at each temperature, as calculated by FactSage. A lower temperature is energetically preferable and protects the crucible, but the liquid area decreases with decreasing temperature. Therefore, the experimental temperature was set at 1673 K, and experiments at 1573 K and 1773 K were also conducted to investigate the effect of temperature variation. In Fig. 2, the average composition of the slag with addition of SiO_2 to the Mn ore at 1673 K is shown. The SiO_2 content of the liquid at MnO saturation is 21.3%, while that at SiO_2 saturation is 52%. Converting the mixing ratio of SiO_2 to the Mn ore, the additions of the upper and lower limits of

the SiO_2 are 15% and 89%, respectively. Here, the mixing ratio to the Mn ore means the ratio between the mass of additives and the Mn ore. Therefore, the mixing ratios of SiO_2 were varied as 30%, 42%, and 54% to investigate the effects of SiO_2 addition.

On the other hand, because the content of Fe oxide in the Mn ore is low, as indicated in Table 1, the amount of metal after reduction is insufficient for accumulating P and, likewise, for good separation between the metal and slag. To solve this problem, C-saturated Fe (pig iron) was added. Because the P content in the metal is decreased during the reduction by the addition of pig iron, the reduction behavior of P will be changed. Therefore, the mixing ratios of pig iron to Mn ore were varied as 10%, 20%, and 40%.

The minimum mixing ratio of graphite powder to reduce MnO, FeO, and P_2O_5 in the Mn ore was approximately 15% of the mass of the Mn ore, calculated from the stoichiometric relation in a given sample. The mixing ratios of graphite powder were thus varied as 5%, 10%, and 20%. The experimental conditions are summarized in Table 2.

Experimental Procedure

To prepare the pig iron, lumps of electrolytic iron were melted with graphite powder at 1473 K in a graphite crucible. The mixing ratio of graphite with iron was 5%. The molten metal was poured onto a cold Cu plate for quenching. After quenching, the pig iron was crushed to a flake size of less than 3 mm and used as a raw material for the

Table 2 List of experimental conditions

	Mixing ratio to Mn ore (mass%)			Temperature (K)	Note
	Graphite	Pig iron	SiO_2		
1	5	20	54	1673	Influence of graphite powder
	10				
	20				
2	10	10	54	1673	Influence of Fe–C (sat.) addition
		20			
		40			
3	10	20	30	1673	Influence of SiO_2 addition
			42		
			54		
4	10	20	54	1573	Influence of temperature
				1673	
				1773	

experiments. The carbon content in the pig iron was around 4%, as analyzed by combustion infrared spectrometer (CIP). The dehydrated Mn ore, flake-sized pig iron, reagent SiO_2, and graphite powder (with particle size smaller than 44 μm) were mixed in the given ratios before the reduction experiments. A total of 5 g of Mn ore was used for each run.

Figure 3 shows the experimental setup. A vertical type of resistance furnace equipped with an alumina reaction tube (inner diameter: 42 mm, height: 1000 mm) and a quartz crucible (inner diameter: 20 mm, height: 85 mm) were used for these experiments. Before charging the sample, the furnace was heated to the target temperature (1573−1773 K), and its atmosphere was controlled with continuously flowing Ar gas (purity: 99.9999%, flow rate: 500 ml/min). For each reduction experiment, mixtures of Mn ore, SiO_2, pig iron, and graphite were loaded into a quartz crucible and then carefully placed in the hot zone of the furnace. Figure 4 shows the heating temperature profiles during the experiments. The mixtures were heated rapidly, and the target temperature was reached within approximately 6 to 8 min. After a given reaction time, the crucible and sample were quickly removed and immediately quenched with water. After quenching, the reduced slag and metal phases were collected separately after crushing, and their compositions were analyzed by ICP–AES. The carbon content of the metal was analyzed using CIP.

Experimental Results

Figure 5 shows a typical image of the cross section of a sample after reduction. A glassy phase of slag with a dark color can be observed, and represents the molten slag formed from
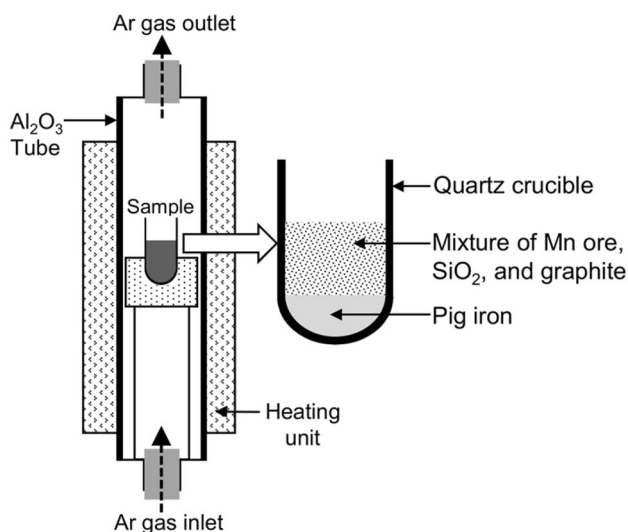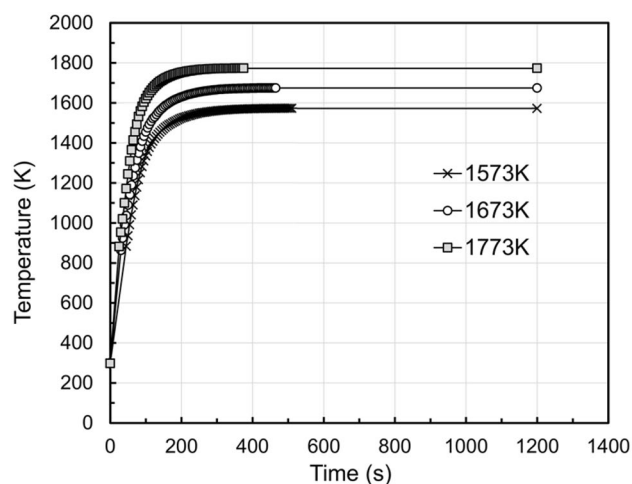

Fig. 4 Profiles of the average temperature in samples during heating

the mixture of the Mn ore and SiO_2. Adjacent to that phase, a light-colored layer is found at the top of the sample. This top layer was found by electron-probe microanalysis (EPMA) to consist of an $MnO–Al_2O_3–SiO_2$ (rich) oxide. The formation of this SiO_2 rich phase is considered due to the dissolution of quartz crucible. As the SiO_2 content in the slag in the top layer was high, only the dark-colored glassy slag was used for ICP–AES analysis.

At the bottom of the crucible, the solidified hot metal can be easily distinguished and separated from the glassy slag. Some residual graphite powder was observed on the surface of the molten slag, even at the lowest mixing ratio of graphite powder.

Typical composition changes in the slag and metal during the reduction are presented in Fig. 6. Regarding the slag composition, most of the Fe in the slag was reduced after 10 min and dissolved in the hot metal, and a decrease in the P content of the slag was observed. The content of P in the slag decreased from the initial 0.23% to 0.03% after 10 min,
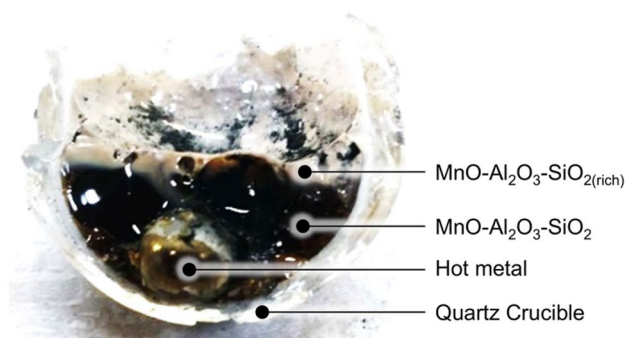

Fig. 3 Schematic diagram of the experimental setup

Fig. 5 Typical image of a sample after 20 min of reduction (mixing ratio: graphite powder: 5%, SiO_2: 54%, pig iron: 20%; temperature: 1673 K). (Color figure online)
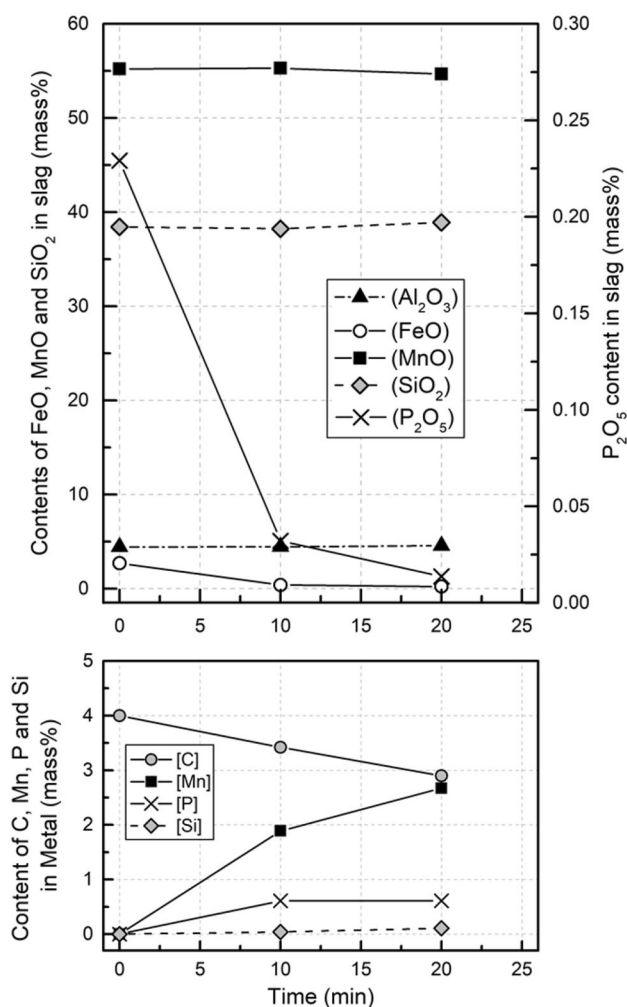
Fig. 6 Typical compositional changes in the slag and metal during reduction (mixing ratio: graphite powder: 10%, SiO_2: 54%, pig iron: 20%; temperature: 1673 K)

insufficient. When the mixing ratio was increased to 10% or more, most contents of the FeO and P_2O_5 in the slag were reduced within 10 min. In the case of the Mn, although the increased addition of graphite powder led to an increase in the Mn content in the metal, the Mn content in the slag was similar for mixing ratios of both 5% and 10%. An obvious decrease in the Mn content in the slag was observed with the addition of 20% graphite. The C content of the hot metal decreased with similar trends and was not affected by the mixing ratio of graphite powder. There may be two reasons for the observed decrease in C content: one is the decrease in C solubility in the metal due to the increased P content, and the other is the consumption of dissolved C by the reduction. More detailed explanations will be discussed later in this paper.

To compare the partition behavior of P and Mn between the slag and metal, the mass balances of P and Mn at given reaction times were calculated. Equation (1) was used to calculate the total mass of slag at a given reaction time using the mass of Al_2O_3 because Al_2O_3 was hardly reduced under the experimental conditions studied.

$$W_{Slag} = 100 \times W_{Al_2O_3}^{Initial}/(mass\%Al_2O_3)_t, \qquad (1)$$

where W_{Slag} is the mass of slag (g), $W_{Al_2O_3}^{Initial}$ is the mass of Al_2O_3 in the initial slag (g), and $(mass\%Al_2O_3)_t$ is the Al_2O_3 content of the slag after reducing for a time t (min). To determine the total mass of metal, a large lump of metal could be easily obtained after the reduction. The weight of the metal was directly measured using a mass scale after each experiment.

The calculated mass balances of P and Mn are shown in Fig. 8. Because the masses of P and Mn before and after the reduction were almost balanced in all cases, vaporization of P and Mn during the reduction was considered negligible. When 5% graphite powder was added, the partition ratio of Mn between the slag and metal was high, but a large amount of P remained in the slag. When the mixing ratio of graphite powder was increased to 10% or more, although the partition ratio of Mn in the slag decreased slightly, the partition ratio of P decreased more significantly. Comparing the results obtained with mixing ratios of 10% and 20%, most of the P in the slag was reduced to the hot metal after 20 min in each case, and the partition ratio of Mn was low enough under both conditions. Therefore, to enhance the reduction of P while suppressing the reduction of Mn, the optimal mixing ratio of graphite powder was considered to be 10%.

Figure 9 shows the influences of the mixing ratios of pig iron on the reduction behavior. As the mixing ratio of pig iron increased, the MnO content in the slag decreased gradually. Specifically, increases in MnO contents in slag were observed at 10 min of reduction for 10% and 20% mixing of pig iron. This is because of the fast reduction of FeO
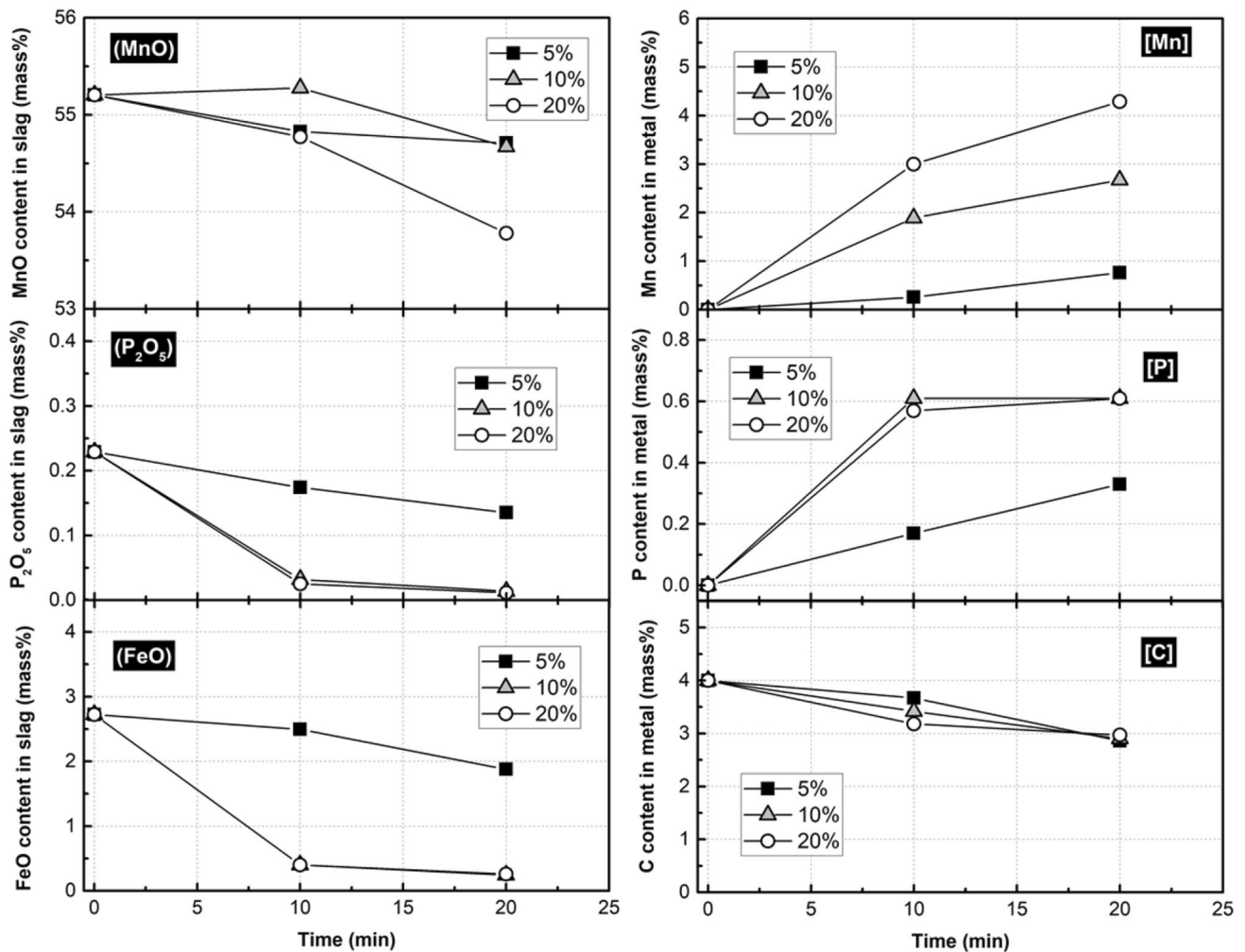
and further decreased to 0.01% after 20 min. As a result, the P content in the metal increased to approximately 0.6% after 10 min and then remained unchanged. In the case of the Mn, the Mn content in the slag barely changed during the reduction, but the Mn content in the metal increased gradually with the reaction time. Thus, the selective reduction of P over Mn was achieved for the Mn ore, as a large part of the P was removed from the slag while the content of Mn in the slag remained unchanged. The SiO_2 content in the slag increased only slightly from 10 to 20 min, primarily due to the dissolution of SiO_2 from the crucible. In the metal phase, the Si content was negligible. The C content in the metal decreased continuously with the reaction time, despite the excess of graphite powder used in the experiment.

The influences of the mixing ratios of graphite powder on the reduction behavior are shown in Fig. 7. At a mixing ratio of 5%, the reductions of both FeO and P_2O_5 were

Fig. 7 Compositional changes in the slag and metal with different mixing ratios of graphite (mixing ratio: SiO_2: 54%, pig iron: 20%; temperature: 1673 K)

when the reduction MnO was still small. The content of P in the slag reached a similar value after 20 min under all conditions. However, with a mixing ratio of 10%, the reduction rate was slower than that for the other cases. The same trend was observed for the change in Fe content. These results indicate that the addition of pig iron affects the reduction kinetics. Both the amounts of P and Mn in the metal were elevated with smaller additions of pig iron. This is because the P and Mn were diluted with the increasing mass of the molten metal. The content of C in the molten metal decreased with the reaction time, but the influence of the mixing ratio of pig iron was negligible.

Figure 10 shows the calculated mass balances of P and Mn for experiments with various mixing ratios of pig iron. When 10% pig iron was added, although the partition of Mn between the slag and the metal was sufficiently high, almost 1/3 of the P remained in the slag after 10 min of reduction. When the mixing ratio of the pig iron was increased to 20%, the partition of P was low, and it decreased little even with further increase in the mixing ratio. Meanwhile, the partition of Mn decreased continuously with an increasing mixing ratio of pig iron. Therefore, to achieve a low partition of P and a high partition of Mn between the slag and metal, 20% addition of pig iron was considered the optimal condition.
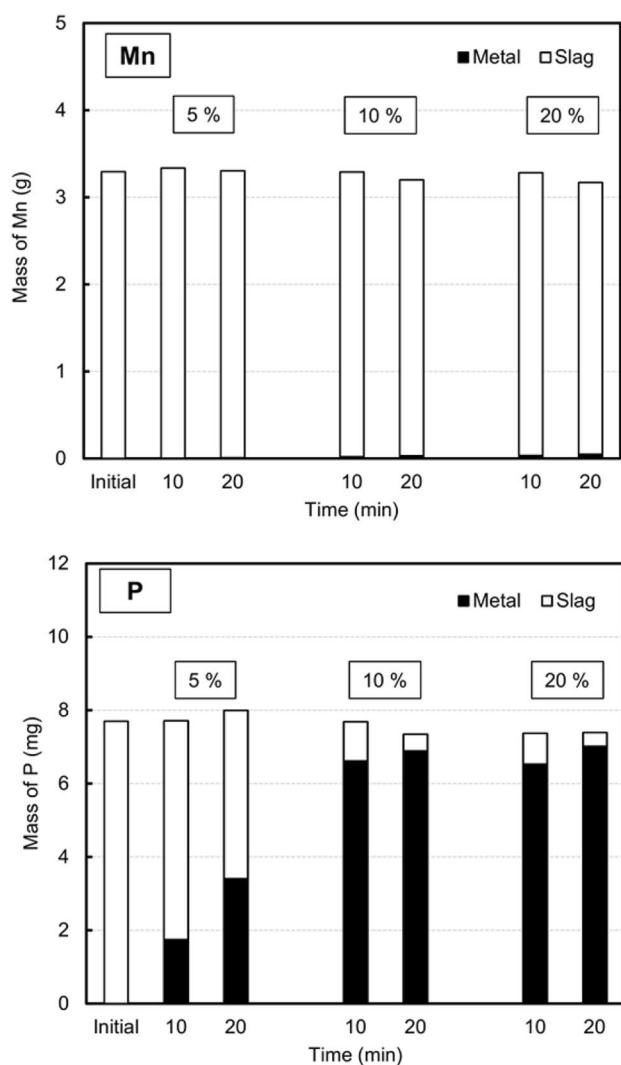
Fig. 8 Calculated mass balances of P and Mn with different mixing ratios of graphite (mixing ratio: SiO_2: 54%, pig iron: 20%; temperature: 1673 K)

Figure 11 shows the influence of the mixing ratio of SiO_2 on the reduction behavior. When the mixing ratio of SiO_2 was small, the increase in SiO_2 content was significant due to dissolution from the crucible. After 20 min, the SiO_2 content in the slag reached a similar value for all conditions, indicating that the slag was close to SiO_2 saturation. Regarding the reduction behavior, although the initial Fe and P contents in the slag differed owing to the different mixing ratios of SiO_2, the reduction of Fe and P in the slag showed similar trends. In the case of Mn, a small mixing ratio of SiO_2 led to its enhanced reduction in the early stage of the experiments.

The calculated mass balances of P and Mn with different mixing ratios of SiO_2 are shown in Fig. 12. With the increasing mixing ratio of SiO_2, the partition of Mn increased, while the partition of P decreased. The addition of SiO_2 affected the activity coefficients of MnO and P_2O_5 in the molten slag, and thus the partitions of P and Mn between the slag and metal were altered. A detailed discussion of this phenomenon will be provided later. Based on the above results, an increase in the mixing ratio of SiO_2 is beneficial for the separation of P and Mn. Therefore, designing a premixture with a SiO_2 content that is close to saturation is considered optimal.

Figure 13 shows the reduction behavior of the slag and the corresponding changes in the metal composition at different temperatures. At temperatures of 1573 K and 1673 K, the content of Mn in the slag barely changed, even after 20 min; however, at 1773 K, the Mn content in the slag decreased. In the cases of Fe and P, the reductions were insufficient at 1573 K, and similar trends were observed at 1673 K. For the metal phase, the changes in the P and C contents were similar, and the Mn content increased with the increasing temperature. Therefore, 1673 K was determined to be the optimal temperature for the selective reduction of P from Mn ore.

Figure 14 shows the calculated mass balances of P and Mn from the reduction results at various temperatures. The partition of Mn decreased slightly with increasing temperature, indicating an enhancement of the reduction of Mn at higher temperatures. For P, the partition of P was high at 1573 K, and decreased with increasing temperature.

Discussion

Contributions of Graphite and Carbon Dissolved in Hot Metal to the Reduction Behavior

The reduction behaviors of P and Mn were affected by the mixing ratios of both the graphite powder and the pig iron. In addition, both results showed that the content of C in the hot metal gradually decreased with the reaction time. To determine the major reaction site and understand the reduction mechanisms of P and Mn, it is necessary to clarify the contributions of the graphite powder and dissolved C in the hot metal to the reduction.

Because the pig iron used in the experiment was C-saturated, the solubility of C in the metal and the measured C content in the metal were compared. The solubility of C in
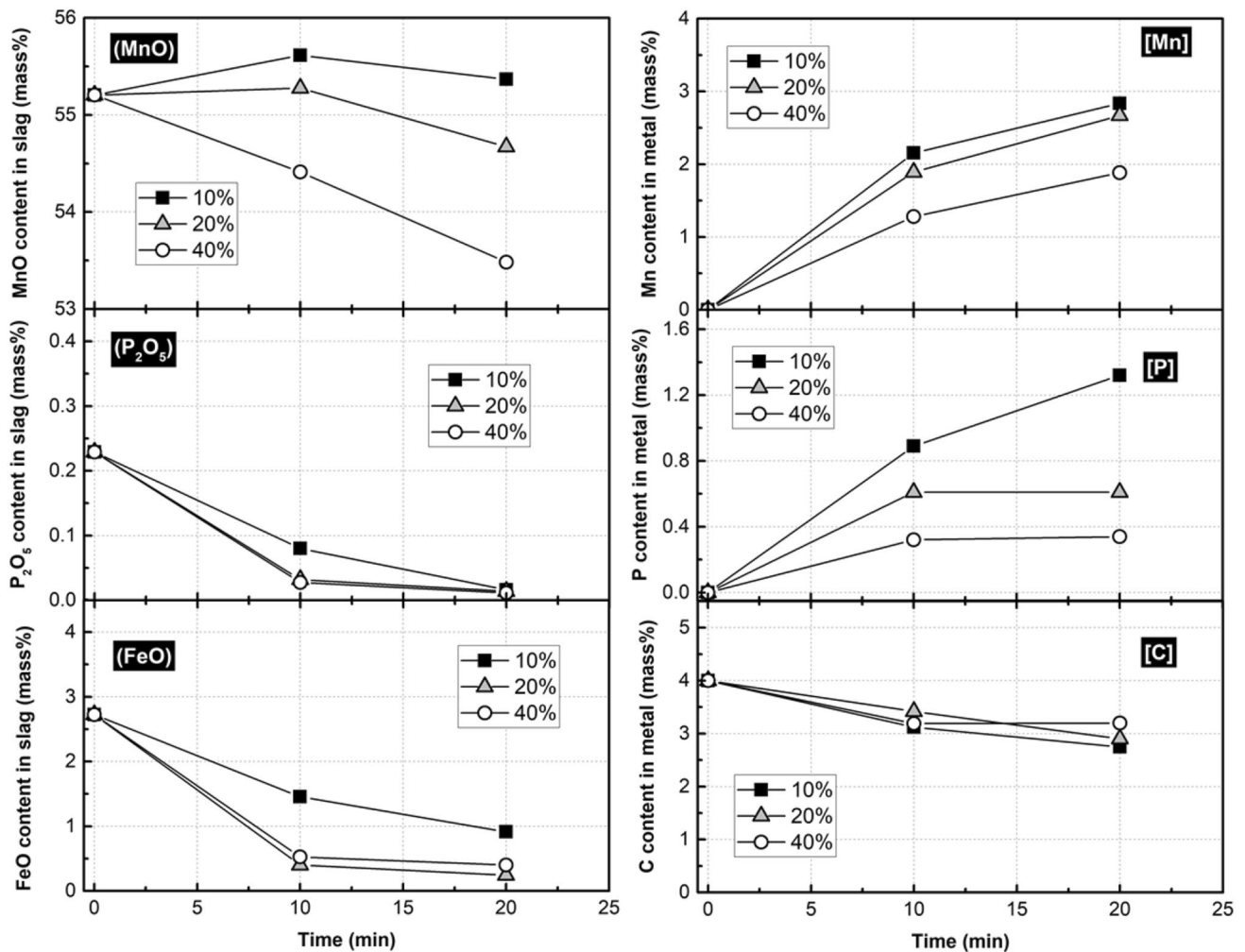
Fig. 9 Compositional changes in the slag and metal with different mixing ratios of pig iron (mixing ratio: graphite powder: 10%, SiO_2: 54%; temperature: 1673 K)

the reduced metal was calculated using Eq. (2), as proposed by the authors in a previous study [20].

$$X_{C[inFe-P-Mn-C(sat)]} = 0.19e^{-(6.09X_P-0.47X_{Mn})} \quad \text{(at 1673 K),}$$
(2)

where X indicates the mole fraction for each element in the metal. Because the molar ratio of Mn in the reduced metal under all experimental conditions was in the range of 0.002−0.03, the relationship between X_P and the C solubility was calculated and compared to the measured C content in the metal after reduction, as shown in Fig. 15. The comparison demonstrates that the measured C content was less

than the C solubility in the alloy, and X_P in the metal had little effect on the C content. When the mixture was rapidly melted, graphite powder floated to the top surface of the molten slag due to its low density, giving the graphite powder little chance to contact the hot metal. Therefore, because the carburization of hot metal by graphite was impeded or slow, the decreased C in the hot metal was considered to be consumed by the reduction reaction.

Based on the above comparison, we find that the reduction occurred at two sites: one is the interface between the hot metal and the molten slag, and the other one is the contact area between the graphite powder and molten slag. To
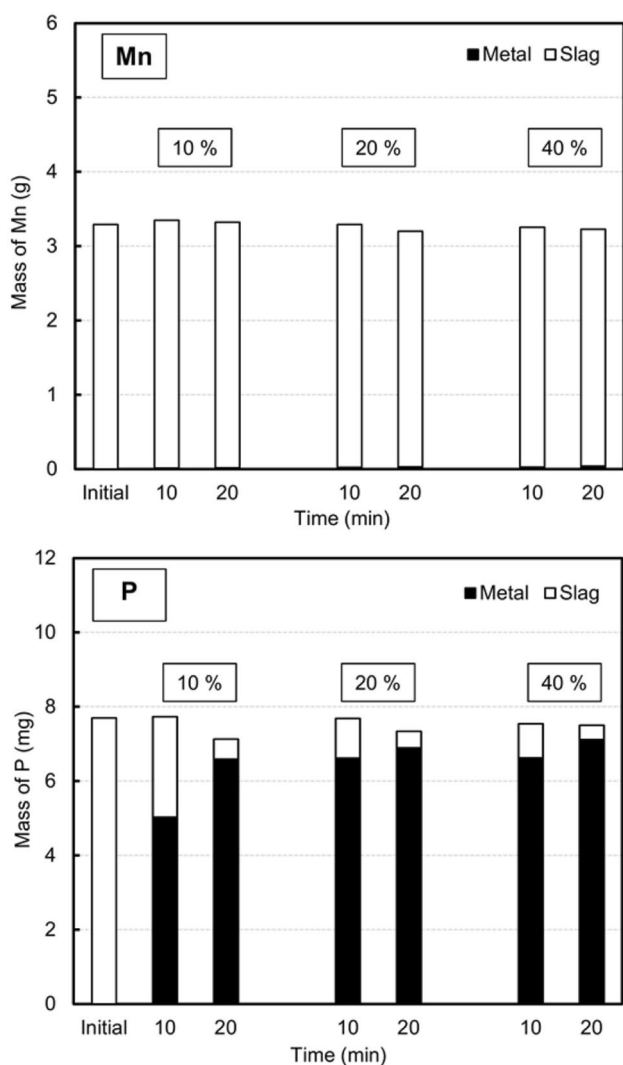
Fig. 10 Calculated mass balances of P and Mn with different mixing ratios of pig iron (mixing ratio: graphite powder: 10%, SiO$_2$: 54%; temperature: 1673 K)

clarify this, the C balances before and after reduction were calculated. In this calculation, the masses of C required for reducing the FeO, MnO, and P$_2$O$_5$ were estimated from the stoichiometry of the reactions, and the changes in the masses of FeO and P$_2$O$_5$ in the slag were used. The mass of C in the hot metal was calculated from the C content and the measured weight of the metal.

The calculated C mass balances before and after reduction are shown in Fig. 16. The amount of graphite powder was not considered because some of it remained unreacted after the experiment. The mass of C required to reduce

the FeO in the slag was greater than that for MnO and P$_2$O$_5$. This is because the total Fe content in the slag was much higher than that of P$_2$O$_5$, and the reduced amount of Mn was small. Compared to the masses of C required to reduce FeO, MnO, and P$_2$O$_5$, the decrease in the mass of C in the hot metal was not enough. Therefore, the graphite powder floating on the slag surface was primarily used as the reductant.

Influence of SiO$_2$ on the Reduction Behavior of P and Mn

To understand the influence of SiO$_2$ addition on the reduction behaviors of P and Mn, the changes in the activity coefficients of both MnO and P$_2$O$_5$ were considered. Figure 17 shows the influence of SiO$_2$ addition on the activity coefficients of P and Mn in the slag. For this figure, the activity coefficients of MnO and P$_2$O$_5$ during the experiments were calculated using FactSage based on the results shown in Fig. 11.

With the increasing addition of SiO$_2$, the activity coefficient of MnO decreased, while that of P$_2$O$_5$ increased. These changes in the activity coefficients led to the thermodynamic preference for selective reduction of P from the slag. Figure 18 shows the effects of the activity coefficient on the distribution ratios of P and Mn between the slag and metal after 10 min of reduction. The distribution ratios (*L*) for P and Mn between the slag and the metal were calculated using Eq. (3).

$$L_P = (\%P)/[\%P], \quad L_{Mn} = (\%Mn)/[\%Mn], \tag{3}$$

where (%A) and [%A] represent the contents of element A in the slag and the metal, respectively.

According to the results shown in Fig. 18, although the slag and metal were not in equilibrium, the distributions of P and Mn between the slag and metal decreased with the increasing activity coefficients. Therefore, SiO$_2$ addition is beneficial for the selective reductions of P over Mn.

Estimation of the Rate-Controlling Step of the Reduction

As the reduction reaction mainly occurred when the slag was in a molten state, the mass transfer in the slag was considered to be the rate-controlling step for the reduction. Because the content of P in the slag was too low, the reduction rate was analyzed using the decreasing rate of Mn in the slag. The rate constant for Mn (k_{Mn}, min^{-1}) was determined using Eq. (4), in which (%Mn)$_a$ and (%Mn)$_b$ indicate the Mn contents in the slag at reaction times, t$_a$ and t$_b$, respectively.
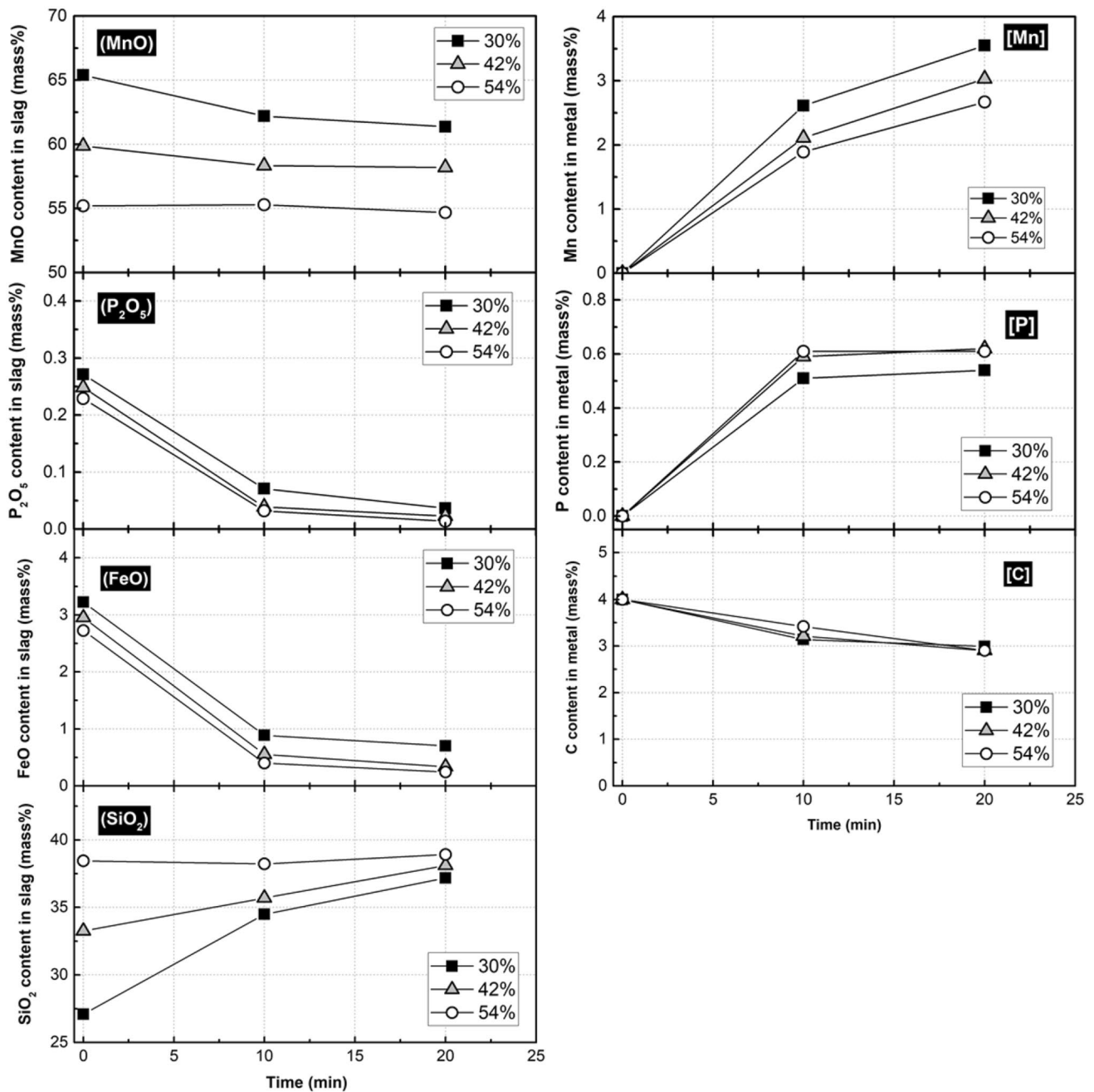
Fig. 11 Compositional changes in the slag and metal with different mixing ratios of SiO_2 (mixing ratio: graphite powder: 10%, pig iron: 20%; temperature: 1673 K)

$$d(\%Mn)/dt = \left[\ln(\%Mn)_a - \ln(\%Mn)_b\right]/(t_a - t_b) = k_{Mn}(\%Mn).$$

(4)

The rate constants for Mn (k_{Mn}) at each temperature were obtained using the results after 10 min of reduction, and the temperature dependence of k_{Mn} was discussed. The results
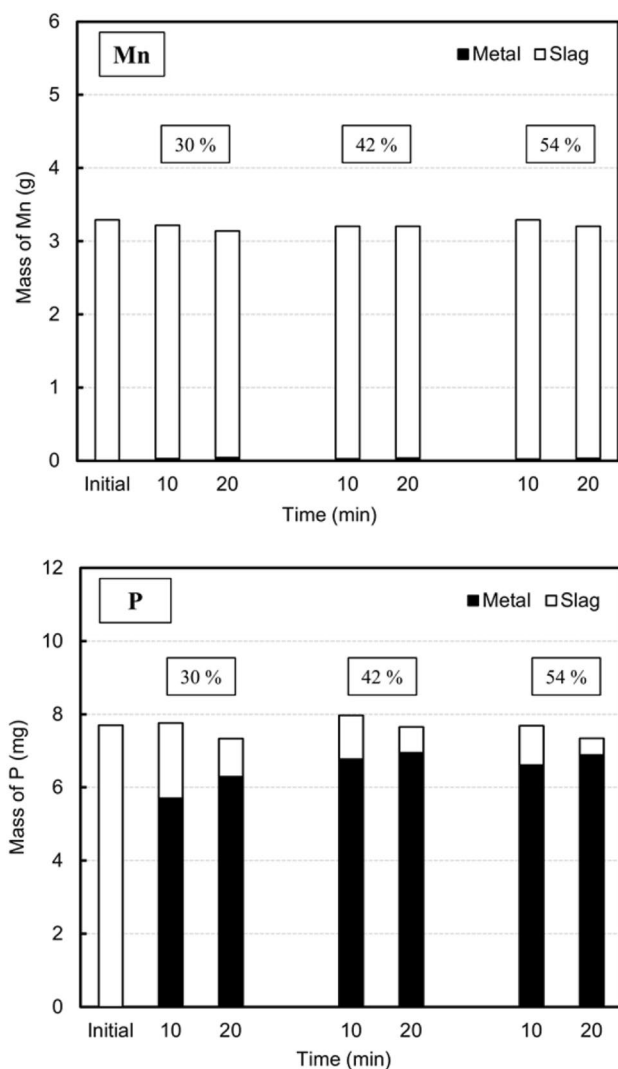
Fig. 12 Mass balance calculations of P and Mn with different mixing ratios of SiO_2 (mixing ratio: graphite powder: 10%, pig iron: 20%; temperature: 1673 K)

are summarized in the form of the Arrhenius equation, as shown in Fig. 19, which was used to determine Eq. (5).

$$\ln k_{Mn} = 24,321/T - 10.58. \tag{5}$$

Using Eq. (5), the activation energy was calculated to be approximately 202 kJ/mol. The activation energy for Mn diffusion in molten slag is about 194.5 kJ/mol [22]. The rate-controlling step can thus be regarded as the diffusion of MnO in the film layer of the slag.

Reaction Mechanism

The changes in the ratios of liquid slag and solid phase during the initial heating stage of the reduction were estimated

using FactSage from the experimental results. For this estimation, the average reaction rate of each component in the slag within 10 min was assumed from Eqs. (6) and (7).

$$W_t^N = W_{ini}^N + \frac{W_{ini}^N - W_{t*}^N}{t*} \times t, (0\ min < t < 10\ mins), \tag{6}$$

$$(N\%)_t = 100 \times \frac{W_t^N}{\sum W_t^i}, \tag{7}$$

where W_t^N is the weight of slag component N at a reaction time t; $t*$ is the reaction time at which the slag composition was analyzed. In this calculation, $t*$ is 10 min, and t is an arbitrary time between 0 min and 10 min. The temperature profile shown in Fig. 4 was used.

The calculated results are shown in Fig. 20. According to the calculation, the liquid-phase ratio gradually increased with time, and approximately 26% of the slag was in the liquid phase after 1 min, when the temperature had reached about 1233 K. After 2 min, the sample was completely melted. As the reduction was caused by the liquid slag, the reaction mode was not the typical carbothermic reduction but is considered a smelting reduction.

The equilibrium relationship between P and Mn in the hot metal after the reduction was estimated using Eq. (8) [23, 24].

$$P_2O_5(l) + 5[Mn] = 2[P] + 5MnO(l)\ \log K = 26950/T + 0.97. \tag{8}$$
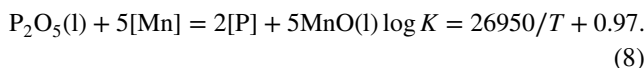
In this estimation, the slag was assumed to be equilibrated with a C-saturated Fe–P–Mn–C alloy. For the activity coefficients of P and Mn in the alloy, Eqs. (9) and (10) were used, as established in a previous study [20].

$$\ln \gamma_{Mn[in Fe-P-Mn-C(sat.)]}^H = -4.72X_P - 0.47X_C, \tag{9}$$

$$\ln \gamma_{P\ [in\ Fe-P-Mn-C\ (sat.)]}^H = -4.72X_{Mn} + 4.26X_P + 6.09X_C, \tag{10}$$

where $\gamma_{Mn\ [in\ Fe-P-Mn-C(sat.)]}^H$ and $\gamma_{P\ [in\ Fe-P-Mn-C(sat.)]}^H$ indicate the Henrian activity coefficients of Mn and P, respectively, in the Fe–P–C_{sat} alloy. The activities of MnO and P_2O_5 were calculated using FactSage with the initial slag compositions. The calculated relationship between the molar ratio of P and Mn is shown in Fig. 21 and compared to the experimental results. The FactSage calculation showed that the activity of P_2O_5 was on the order of 10^{-16}, while that of MnO was on the order of 10^{-1}. As shown in Fig. 21, the experimental results are located close to the assumed equilibrium relation.
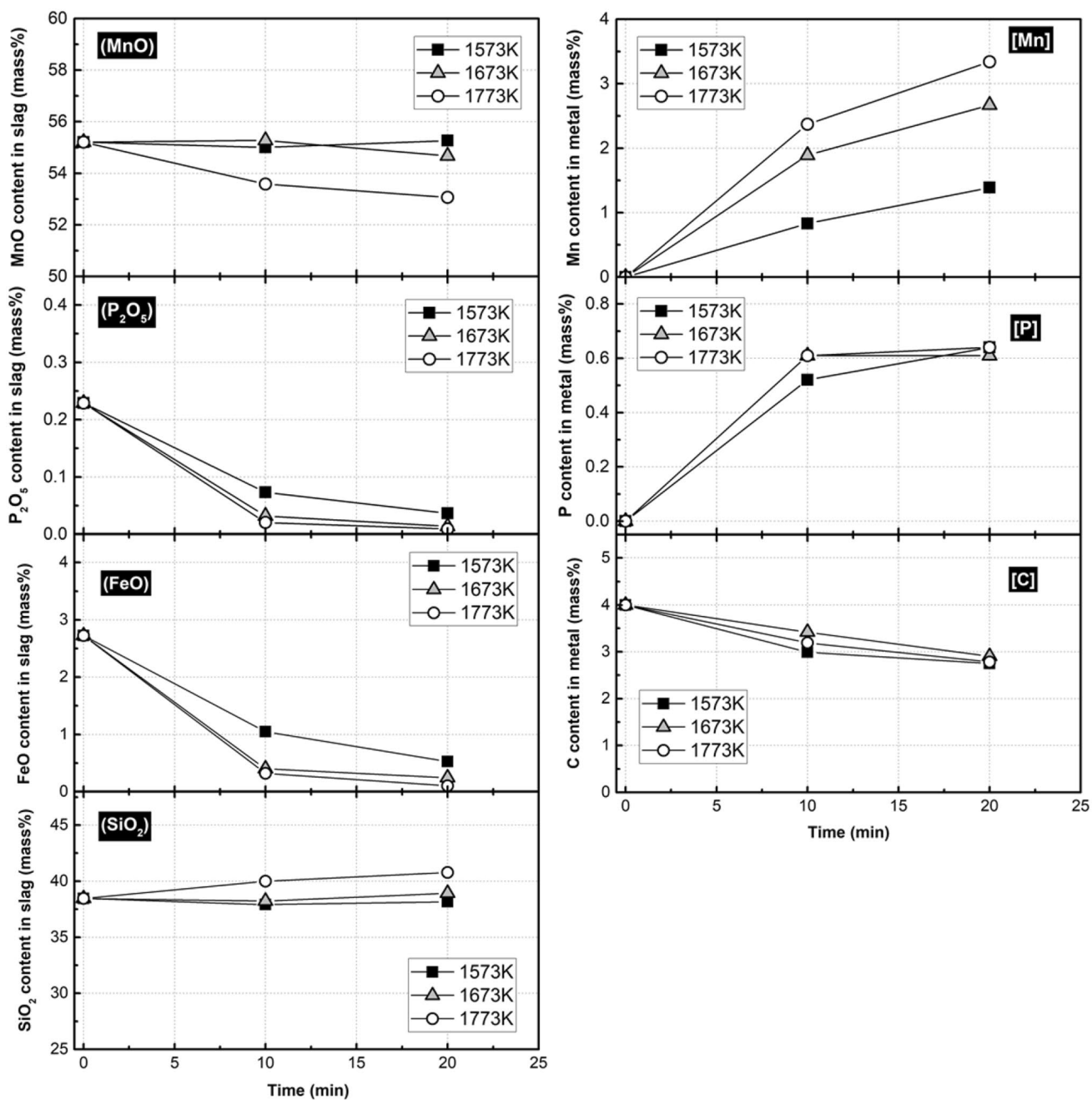
Fig. 13 Compositional changes in the slag and metal at different temperatures (mixing ratio: graphite powder: 10%, SiO$_2$: 54%, pig iron: 20%)
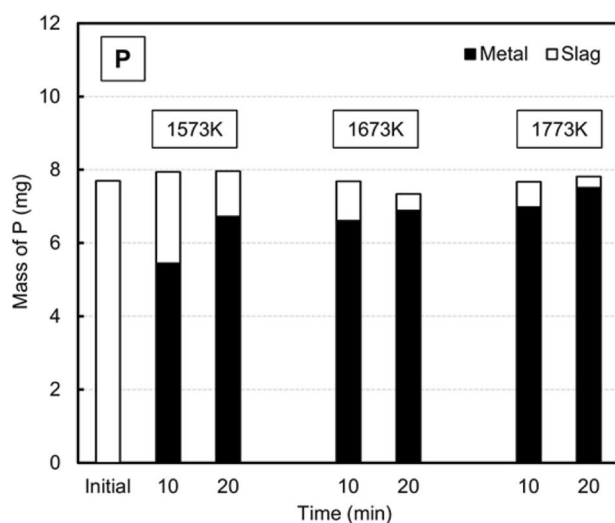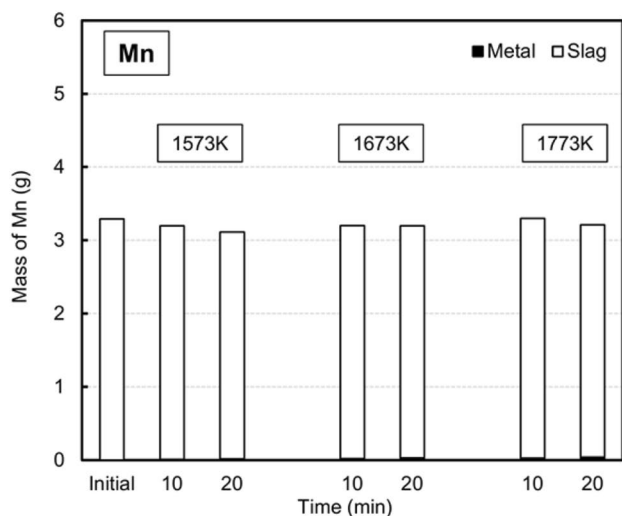
Fig. 14 Mass balances of P and Mn at different temperatures (mixing ratio: graphite powder: 10%, SiO_2: 54%, pig iron: 20%)

Therefore, it is concluded that the reductions of MnO and P_2O_5 occurred mainly in the liquid slag.

Possibility for the Production of a Low-P Ferromanganese Alloy

The purpose of the selective reduction of P from Mn ore was to produce a ferromanganese alloy with low phosphorus content. The possibility of producing this high grade of ferromanganese from the slag obtained after the removal of P with a subsequent reduction was evaluated by calculation. In this calculation, the production of the high-carbon ferromanganese alloy was considered, and thus the target content of Mn in the product alloy was assumed to be 80% and
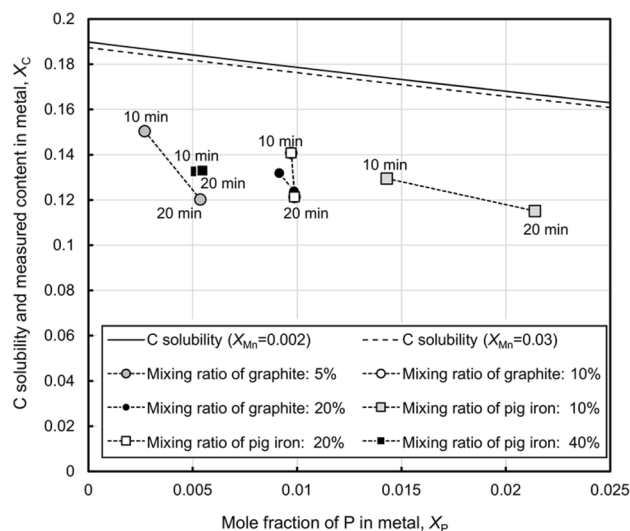

Fig. 15 Difference between the C contents measured in hot metal after reduction and the calculated C solubility in the Fe–P–Mn–C alloy

the carbon content was 7.0%. Because the ferromanganese alloy was generally produced through a smelting reduction process, the yield ratios of Fe, P, and Mn in the smelting reduction were assumed to be 98% [25], 60% [25], and 90% [26], respectively, based on the available reference data. The slag composition after 20 min of reduction for Mn ore under optimal conditions was used in the calculation. For comparison, the reduction of the original ore without the selective reduction treatment was also calculated. Table 3 summarizes the calculated compositions of the ferromanganese alloys.

When the original Mn ore was used directly, the content of P in the ferromanganese alloy was 0.32%. On the other hand, with use of the slag with P removed obtained from the selective reduction, the P content in the alloy was less than 0.05%. Based on this result, the selective reduction of P from Mn ore is considered a valid option to produce high-grade ferromanganese alloys with low P content.

It should be noted that some metal droplets may be trapped within the molten slag after reduction; if these metal droplets contain a high content of P, the P content in the ferromanganese alloy may have higher values than those listed in Table 3. However, the sum of the masses of P in the metal and in the reduced slag balanced well with the input
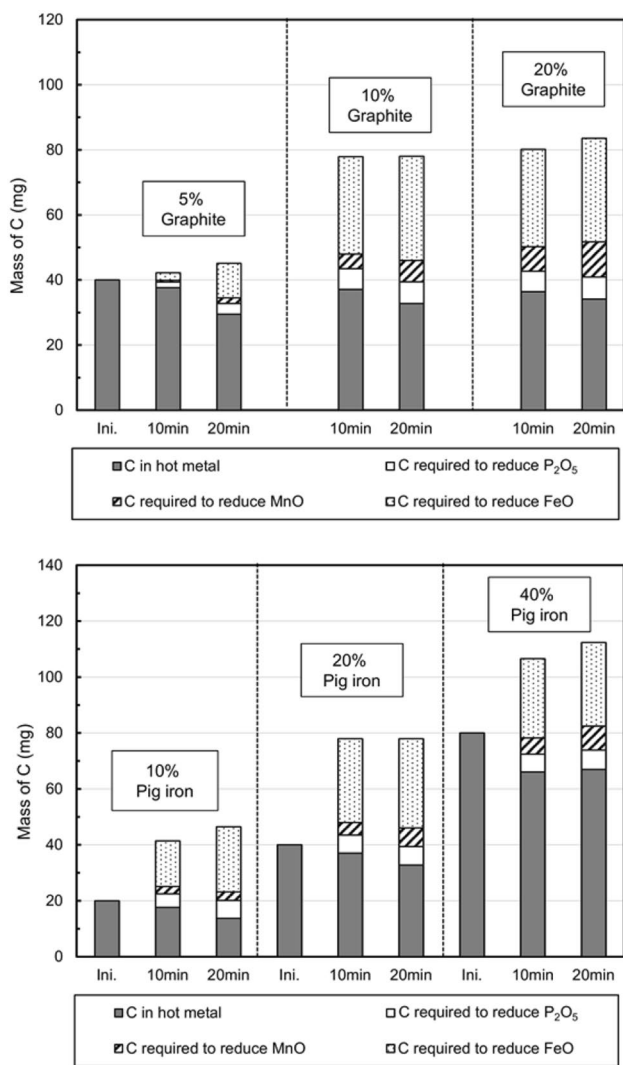
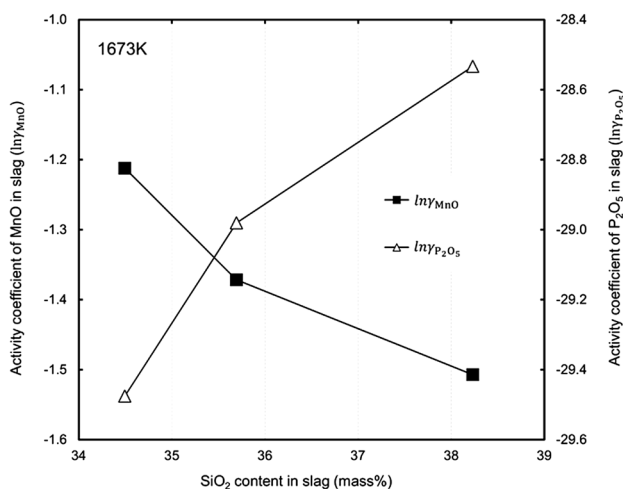Fig. 16 Mass balance of carbon for each experimental condition

Fig. 17 Influence of SiO$_2$ content on the activity coefficients of MnO and P$_2$O$_5$
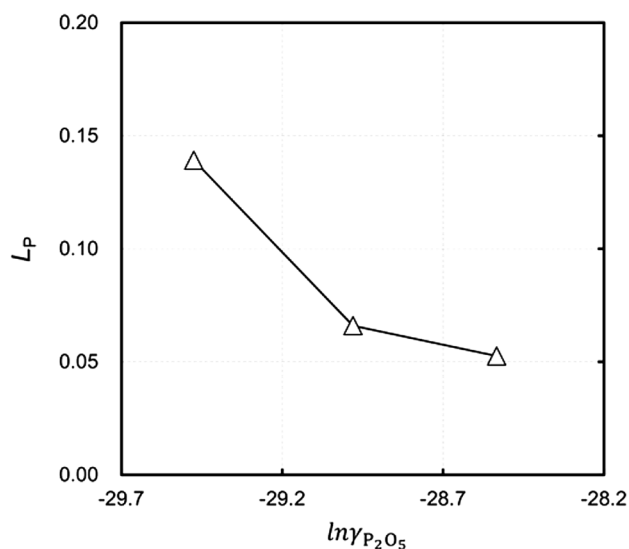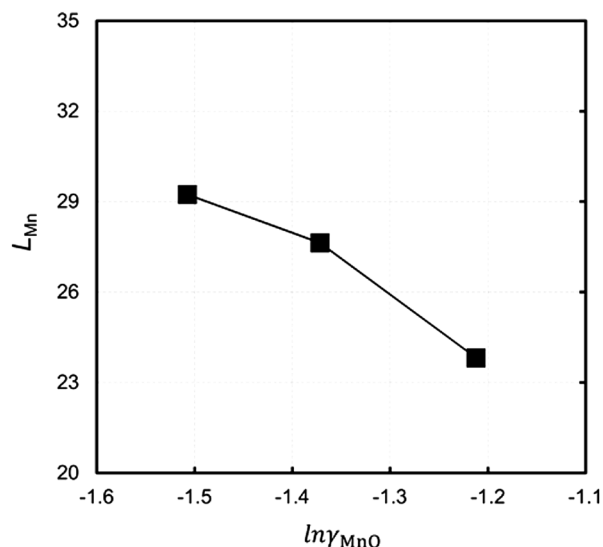

Fig. 18 Influences of the activity coefficients on the distribution ratios of P and Mn

mass of P, with a small deviation. Therefore, there is a low chance that the uncollected metal droplets trapped in the slag would carry a large enough amount of P to influence the P content of the ferromanganese after the secondary reduction.

Conclusion

A selective reduction technique for P was applied to a kind of Mn ore in this study. The purpose was to decrease the P content of the original ore, and thus to provide a method for the production of ferromanganese with a low P content from
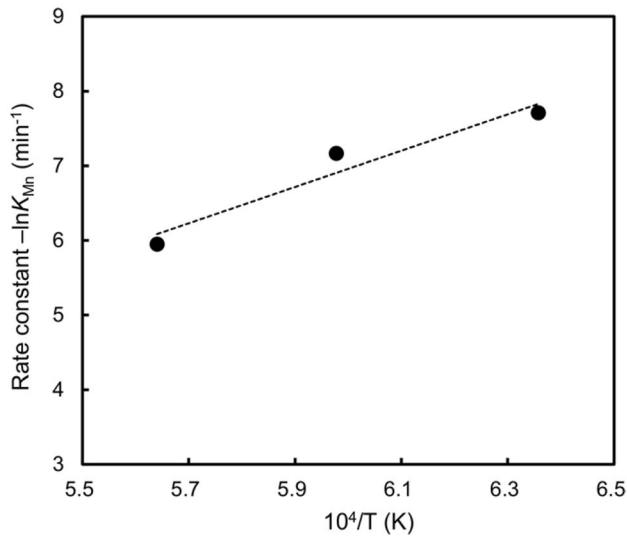
Fig. 19 Temperature dependence of the rate constant for Mn (k_{Mn}), calculated using Eq. (4)
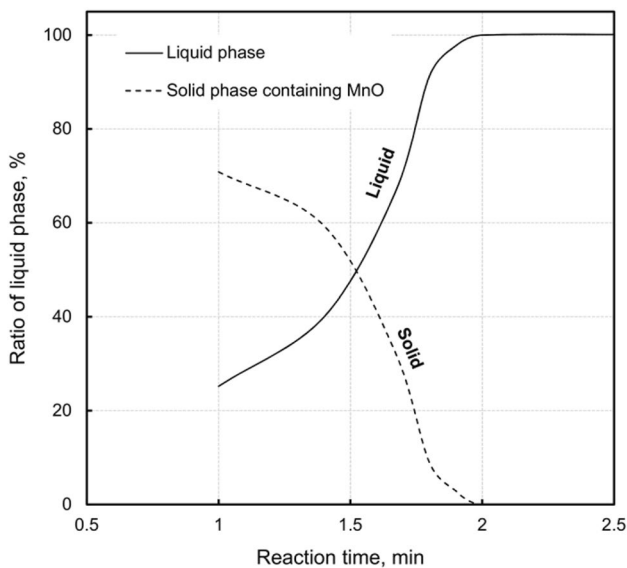

Fig. 21 Comparison between the calculated equilibrium compositions and the experimental results

Fig. 20 Estimated phase ratios of the liquid and solid phases during the initial period of the reduction

Table 3 Expected P contents in ferromanganese alloys produced from different raw materials (mass%)

	Mn ore (raw)	Reduced slag (from Mn ore)
Raw material		
T. Mn	52.0	42.0
T. P	0.14	0.006
T. Fe	3.4	0.5
Ferromanganese (estimated)		
Mn	80.0	80.0
Fe	Bal.	Bal.
C	7.0	7.0
P	0.323	0.017

a normal grade of Mn ore. Through reduction experiments, some main conclusions have been drawn as follows:

(1) By adding SiO_2 as a slag modifier to make an acidic slag with a low melting temperature and adding graphite and pig iron as a reductant and receiver, respectively, the selective reduction of P without reduction of Mn was achieved for Mn ore.
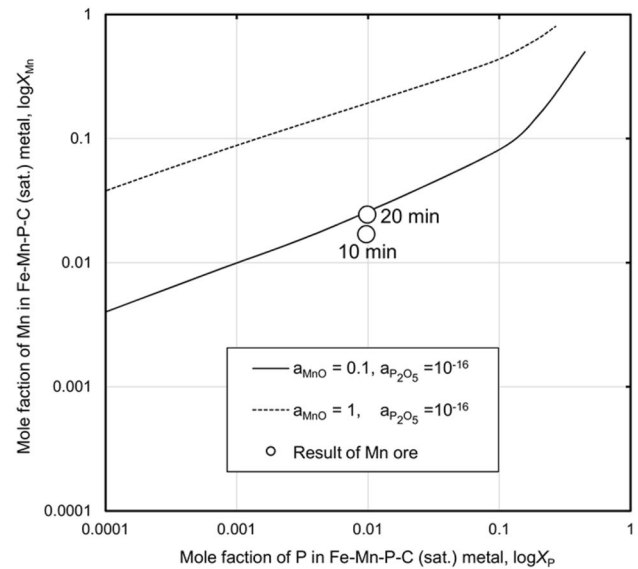
(2) For the Mn ore, the influences of the different mixing ratios of graphite powder, pig iron, and SiO_2 on the reduction behavior were investigated. The results showed that both the graphite powder and the pig iron contributed to the reduction, and the reductions of P and Mn were enhanced with the addition of more graphite powder and pig iron. To suppress the reduction of Mn in the slag while obtaining a high removal ratio of P from the slag, the optimal mixing ratios of graphite and pig iron were determined to be 10% and 20%, respectively. In addition, some discussion was

presented attempting to understand the contributions of graphite power and the dissolved C in pig iron to the reduction.

(3) The increasing SiO_2 addition suppressed the reduction of Mn and enhanced the reduction of P. Because the slag needed to be in a liquid state, the optimal mixing ratio of SiO_2 at 1673 K was determined to be 54% for Mn ore. The effects of SiO_2 on the reduction behaviors of P and Mn were discussed based on the changes in the activity coefficients and distribution ratios.

(4) When the reduction was conducted at 1573 K, the results for Mn ore indicated that the reductions of both Fe and P from the slag were insufficient, while the reduction at a high temperature of 1773 K increased the loss of Mn from the slag to the metal. Therefore, the optimal temperature for reduction was determined to be 1673 K.

(5) When the slag obtained after the selective reduction of both Mn ores was used in the smelting reduction process to produce ferromanganese alloy, a significant decrease in the P content of the ferromanganese was estimated through a mass balance calculation. Therefore, the selective reduction of P from Mn ore is considered a valid option to produce high-grade ferromanganese alloys with low P content.

References

1. Olsen SE, Tangstad M, Lindstad T (2007) Production of manganese ferroalloys. SINTEF and Tapir Academic Press, Trondheim
2. Seetharaman S, Mclean A, Guthrie R, Seetharaman S (2014) Treatise on process metallurgy. Industrial processes, vol 3. Elsevier, Amsterdam, pp 477–532
3. Gasik M (2013) Handbook of ferroalloys, theory and technology. Butterworth-Heinemann, Elsevier, Amsterdam, pp 221–266
4. Fonstein N (2015) Advanced high strength sheet steels, physical metallurgy, design, processing, and properties. Springer, New York, pp 369–392
5. Sherstyuk AA, Shulte YA (1963) Effect of phosphorus on the properties of high-manganese steel. Met Sci Heat Treat 5:271–273
6. Chaudhary PN, Goel RP, Roy GG (2001) Dephosphorisation of high carbon ferromanganese using $BaCO_3$ based fluxes. Ironmak Steelmak 28(5):396–403
7. Fujita M, Katayama H, Yamamoto A, Matsuo M (1988) Dephosphorization of Fe–Mn–C alloy with $BaCO_3$. Tetsu-to-Hagané 74(5):816–822
8. Shim SC, Tsukihashi F, Sano N (1993) Thermodynamic properties of the BaO–MnO flux system. Metall Mater Trans B 24(2):333–337
9. Watanabe Y, Kitamura K, Rachev IP, Tsukihashi F, Sano N (1993) Thermodynamics of phosphorus and sulfur in the BaO–MnO flux system between 1573 and 1673 K. Metall Mater Trans B 24(2):339–347
10. Liu X, Wijk O, Selin R, Edström JO (1998) Effects of additives in $BaO–BaF_2–MnO$ slag on phosphate and manganese capacities. ISIJ Int 38(1):36–45
11. Kim DY, Kim HS, Jung SM (2015) Production of (Mn, Fe)-carbide containing low phosphorus by carbothermic reduction of Mn oxide and Fe oxide. ISIJ Int 55:504–512
12. Kononov R, Ostrovski O, Ganguly S (2009) Carbothermic solid state reduction of manganese ores: 1. Manganese ore characterization. ISIJ Int 49:1099–1106
13. Kononov R, Ostrovski O, Ganguly S (2009) Carbothermic solid state reduction of manganese ores: 2. Non-isothermal and isothermal reduction in different gas atmospheres. ISIJ Int 49:1107–1114
14. Rao GV, Acharya BC, Murty BVR, Mohanty JN, Swamy YV, Chattopadhay P, Tripathy AK (1998) Removal of phosphorus and enrichment of manganese from a complex ferruginous manganese ore. Phys Sep Sci Eng 9(2):109–123
15. Acharya BC, Rao DS, Sahoo RK (1997) Mineralogy, chemistry and genesis of Nishikhal manganese ores of South Orissa, India. Miner Depos 32(1):79–93
16. Hils G, Newirkowez A, Kroker M, Grethe U, Schmidt-Jürgensen R, Kroos J, Spitzer KH (2015) Conventional and tailored Mn-bearing alloying agents for the production of high manganese steels. Steel Res Int 86(4):411–421
17. Shin D, Gao X, Ueda S, Kitamura S (2017) Separation of phosphorus and manganese in dephosphorization slag by carbothermic reduction. CAMP-ISIJ 30:248
18. Shin D, Gao X, Ueda S, Kitamura S (2017) Selective recovery of phosphorus and manganese from steelmaking slag by carbothermic reduction. In Proceeding 5th international slag valorization symposium, K. U. Leuven, Belgium, pp 161–164
19. Shin D, Gao X, Ueda S, Kitamura S (2018) Selective recovery of P and Mn from steelmaking slag by carbothermic reduction. In 9th international symposium on high-temperature metallurgical processing, Springer, Cham, pp 305–311
20. Shin D, Gao X, Ueda S, Kitamura S (2018) Measurement of activity coefficients of Mn and P in C saturated Fe–Mn–P alloy. CAMP-ISIJ 31:127
21. Shin D, Gao X, Ueda S, Kitamura S (2018) Influence of melting behavior on the selective reduction of phosphorus from steelmaking slag. CAMP-ISIJ 31:680
22. Fontana A, Segers L, Winand R (1981) Electrochemical measurements in silicate slags containing manganese oxide. Can Metall Q 20(2):209–214
23. Turkdogan ET, Pearson J (1953) Activities of constituents of iron and steelmaking slags. JISI 12:398–402
24. Suito H, Inoue R (1984) Thermodynamic considerations on manganese equilibria between liquid iron and FeO–MnO–MO_x ($MO_x = PO_{2.5}$, SiO_2, $AlO_{1.5}$, MgO, CaO) slags. Tetsu-to-Hagané 70(6):533–540
25. Eissa M, Ghali S, Ahmed A, El-Faramawy H (2012) Optimum condition for smelting high carbon ferromanganese. Ironmak Steelmak 39(6):419–430
26. Groshkova AL, Polulyakh LA, Travyanov AY, Dashevskii VY, Yusfin YS (2007) Phosphorus distribution between phases in smelting high-carbon ferromanganese in the blast furnace. Steel Transl 37(11):904–907